ELSEVIER

Chemical Geology 224 (2005) 55–68

CHEMICAL GEOLOGY
INCLUDING
ISOTOPE GEOSCIENCE

www.elsevier.com/locate/chemgeo

Geochemistry of Champagne Hot Springs shallow hydrothermal vent field and associated sediments, Dominica, Lesser Antilles

Kevin T. McCarthy, Thomas Pichler *, Roy E. Price

University of South Florida, Department of Geology, 4202 E. Fowler Avenue Tampa, FL 33620-5201, United States

Received 11 October 2004; accepted 4 July 2005

Abstract

The Champagne Hot Springs (CHS) shallow submarine hydrothermal system is located along the submerged flank of the Plat Pays volcanic system on the southwest section of the island of Dominica, Lesser Antilles. We have conducted a detailed geochemical study of the hydrothermal system, with the objectives to investigate the source of the hydrothermal fluids and gases, their effect on sediment and precipitate chemistry, as well as comparing the submarine vent chemistry with nearby on-land hydrothermal vents. Finally, we compare our findings to previous preliminary data from CHS, and compare sediment chemistry to that of average Caribbean sediments. We also report on a newly discovered area of submarine hydrothermal venting, located approximately 40 m to the north of CHS. This area consists of hydrothermally altered areas of sand that contain abundant coatings of hydrous ferric oxides (HFO) on sediment grains.

Geochemical and mineralogical analyses of vent waters, pore waters, gases, sediments and precipitates reveal that the vent fluids consist of a mixture of entrained seawater and meteorically derived hydrothermal fluid in varying proportions. Vent fluids are depleted in Br^-, SO_4^{2-}, Cl^-, Na^+, K^+, and Sr^{2+} relative to ambient seawater. These species are all positively correlated with Mg^{2+}, which is also depleted relative to seawater. Boron, Fe, As, Sb, Mn, Si and Li are all enriched relative to ambient seawater. Pore waters in the hydrothermally altered sand patches have essentially the same chemistry. Mixing between Fe^{2+} rich vent fluids and seawater causes rapid oxidation of Fe^{2+} to insoluble Fe^{3+} and leads to precipitation of HFO at the vent site and subsequent formation of hydrothermally altered sand patches. The elevated concentrations of As and Sb in the precipitates and sediments relative to average Caribbean seafloor sediments reflect adsorption by HFO. Gas samples from the vent site are typical arc-type gases and have both meteoric and magmatic signatures.
© 2005 Elsevier B.V. All rights reserved.

Keywords: Dominica; Champagne Springs; Shallow-water hydrothermal venting; Hydrous ferric oxides

1. Introduction

Shallow submarine hydrothermal sites occur along the flanks of volcanic islands and the tops of seamounts (Dando and Leahy, 1993; Heikoop et al., 1996; Hodkinson et al., 1994; Pichler and Dix, 1996; Pichler et al., 1999a; Sedwick and Stüben, 1996). Research on these systems is important because they are considered modern analogs for epithermal metal deposits, they may have significant impact on the chemistry and ecology of the surrounding environment, and knowledge gained from these systems can help our understanding of elemental cycling and sediment alterations, which in turn may be applied to deep-water systems and the

* Corresponding author. Tel.: +1 813 974 0321; fax: +1 813 974 2654.
E-mail address: Pichler@shell.cas.usf.edu (T. Pichler).

0009-2541/$ - see front matter © 2005 Elsevier B.V. All rights reserved.
doi:10.1016/j.chemgeo.2005.07.014

genesis of ore deposits. In addition, the shallow-water hydrothermal systems associated with the submerged flanks of island arc volcanoes are ideal environments to study the differences between subaerial and submarine venting and the transition between the two.

Champagne Hot Springs (CHS) is a shallow submarine hydrothermal area located in the southwest section of the island of Dominica, Lesser Antilles (Fig. 1). While preliminary data exists for this system (Johnson and Cronan, 2001), this is the first time it has been researched in detail. We have investigated this hydrothermal system with the objective of providing a detailed geochemical analysis and interpretation of the hydrothermal fluids, gases, sediments and precipitates. We also describe a newly discovered hydrothermal area consisting of warm sand and iron oxide coatings on sand grains just to the north of the main vent area. Specifically, this research addresses the following questions:

1. What is the source of the hydrothermal fluids and gases?
2. What are the geochemical effects of shallow hydrothermal submarine venting on pore fluids, sediments and precipitates?

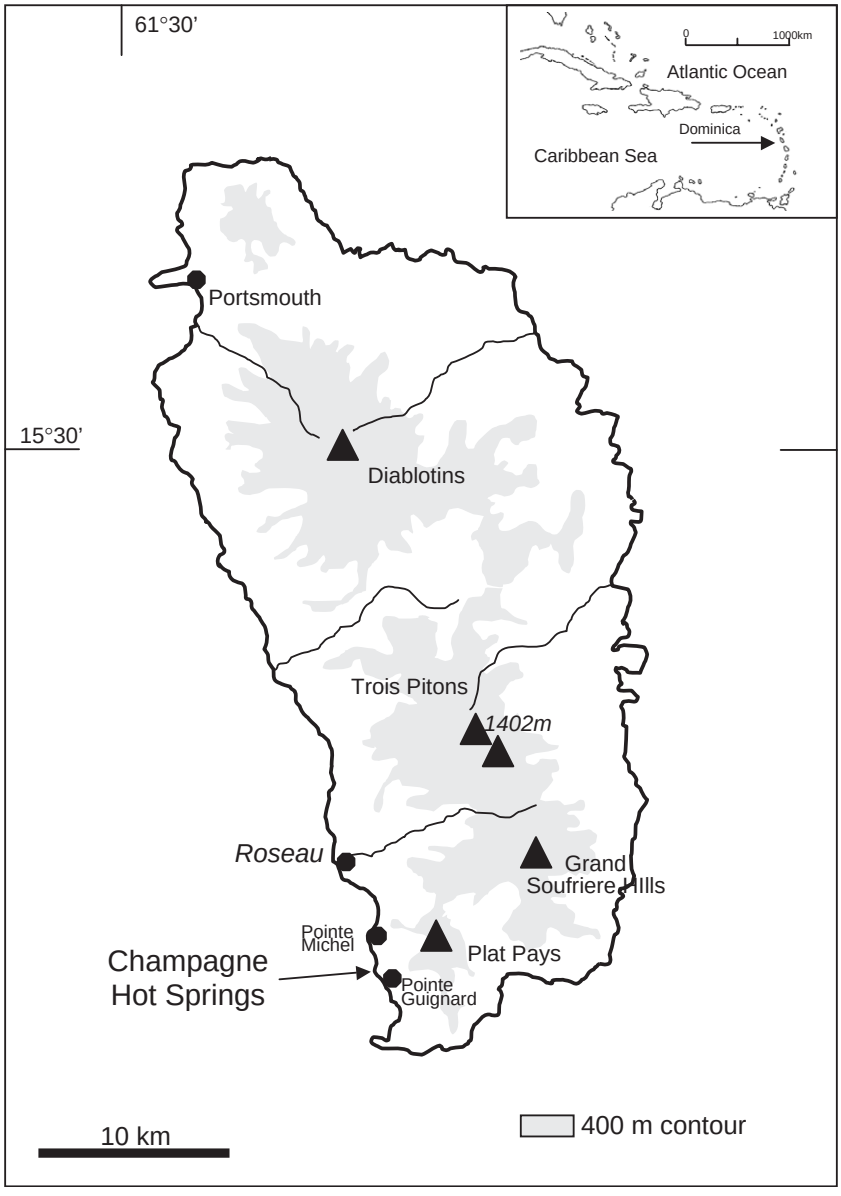

Fig. 1. Map of Dominica showing the location of Champagne Hot Springs (modified from UNEP/IUCN, 1988).

3. How do vent fluids from CHS compare with nearby subaerial vents?
4. How are the hydrothermal sand patches related to the CHS?

1.1. Location and geological setting

Dominica is one of the islands that comprise the Lesser Antilles archipelago, one of only two active island arc systems in the Atlantic Ocean. The Lesser Antilles are a double island-arc system that converges to form a single chain of islands just to the southeast of Dominica (Fink, 1972; Martin-Kaye, 1969). Dominica is located on the inner arc and is one of the Caribbean islands where volcanic activity has been restricted to the Pliocene–Quaternary periods. Beginning in the middle Pliocene, basaltic–andesitic shield volcanoes were emplaced on Miocene age volcanic rocks that form the basal portion of Dominica (Lindsay et al., 2003). During the Pleistocene, composite andesitic volcanoes were superimposed upon these middle Pliocene shield volcanoes. These form a north/south trending chain of volcanoes that include Morne Diables, Morne Diablotins, Morne Anglais, and Morne Plat Pays (Fig. 1). Approximately 30,000 years ago an eruption formed the voluminous Roseau ignimbrite, which was followed by a shift towards more effusive type volcanism and the formation of numerous pelean andesite/dacite dome complexes. These latter events are the source for the dominant medium-K calc-alkaline andesites found in the Champagne Hot Springs area (Sigurdsson and Shepherd, 1974). The emplacement of these pelean dome complexes has formed a steep topography in the CHS area, with elevations rising to over 500 m at less than 800 m inland from the CHS vent site (Lindsay et al., 2003). The erosion of these steep cliffs forms conglomerates of previously emplaced pyroclastic block and ash flows. Champagne Hot Springs is located on the southwest flank of the Morne Plat Pays volcanic complex, on the southern tip of Dominica, approximately 2 km south of the coastal community of Pointe Michel and just offshore from the landmark of Pointe Guignard (Fig. 1).

1.2. Field observations

Submarine hydrothermal venting occurs at Champagne Hot Springs in 1–5 m water along the submerged flank of the Plat Pays volcanic complex. The vent field extends approximately 40 m seaward and is 22 m at its maximum width, for a total area of 880 m^2 (Fig. 2). Venting occurs along two east–west trending fissures in the lava rock, demonstrating possible structural control on vent locations and distribution. Recent studies correlate vent locations to on-land fractures associated with the collapse scarp surrounding the Soufriere depression (Lindsay et al., 2003). Two types of venting are observed: (1) Focused discharge of a clear fluid occurring at discrete ports, 2–6 cm in diameter; and (2) Dispersed or diffusive discharge of vent fluid and streams of gas bubbles emerging directly through the fractured volcanic rocks and unconsolidated sediment (Fig. 3a). Venting through sediment can be intermittent, with shifts in location on the order of a few centimeters.

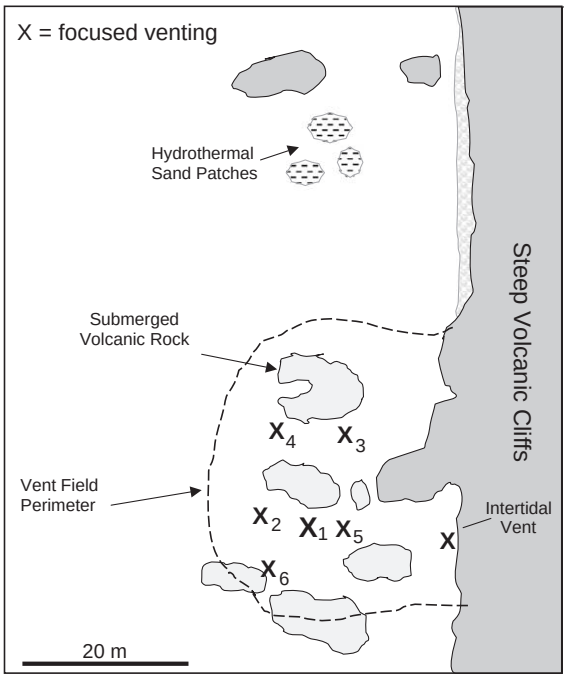

Fig. 2. Map of the Champagne Hot Springs vent field, including the location of colored sand patches.

Six locations of focused hydrothermal venting were identified at CHS, along with diffuse venting and abundant gaseous discharge throughout the area (Fig. 2). Vent 2 is the largest (approximately 6 cm in diameter) and also has the highest flow rate (approximately 0.4 L/min). Vents 1 and 3 are 3–4 cm in diameter, with flow rates similar to but slightly less than Vent 2. Vents 4, 5 and 6 all have smaller orifices (1–2 cm) and discharge fluids at considerably slower rates than vents 1, 2, and 3. One intertidal vent (CSL 1) was also sampled at Champagne Hot Springs. The vent is approximately 2 cm in diameter and discharges fluid immediately adjacent to the high tide water line, being submerged at high tide and exposed at low tide. Discharge occurs through sand to cobble sized volcanic sediment with extensive precipitation of orange to brown-black HFO.

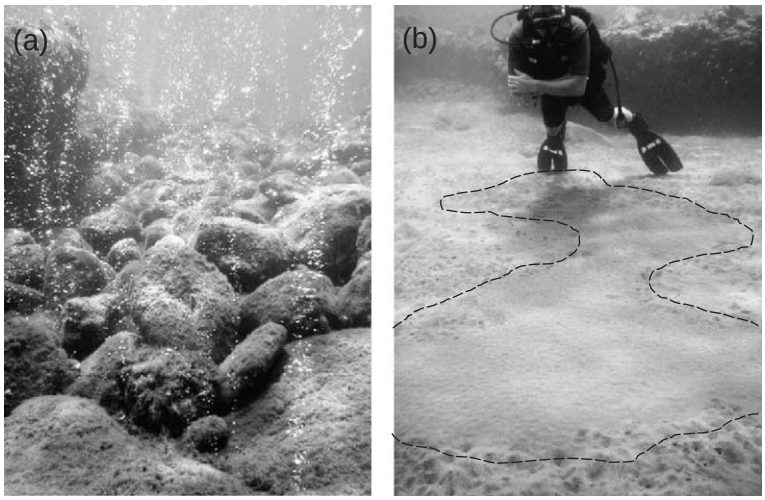

Fig. 3. (a) Diffusive discharge of gas bubbles through fractured volcanic rock (see diver in b for scale). (b) Hydrothermal sand patch (dashed outline) at sediment/seawater interface. Note the difference in bioturbation between the colored and "normal" sediment.

Hydrous ferric oxide (HFO) precipitates are present in the submarine Champagne Hot Springs area and are limited to the immediate vicinity of venting. At distances greater than approximately 2 m, they are only present as a thin orange coating on the volcaniclastic sediments. Closer to vent orifices HFO precipitates occur in layers up to 5 cm thick. The precipitates range in color from bright orange to dark brown.

Approximately 40 m north of the main vent field, the seafloor changes from exposed volcanic rock to mostly unconsolidated volcaniclastic sediment that is approximately half a meter thick. Here, discrete, irregular patches of hydrothermally altered sand are present (Fig. 3b). The patches vary in size from a few centimeters to several meters in diameter. The sediment in these patches is coated with a thin orange veneer similar to that found on the sediments and rocks within the vent field. Coring of these patches revealed that the orange coating extends to a depth of about 15 cm. Repeated excursions to the site indicate that the shape and abundance of these patches varies over time. These changes appear to be seasonal, with patches being more prevalent during the rainy season, and may be linked to fluctuations in discharge volume.

2. Methods

2.1. Field

Field work was conducted over a period of 6 days and consisted of sampling vent fluids, pore fluids, sediments and precipitates. Vent fluid temperatures were measured underwater with a Forestry Suppliers waterproof digital thermometer at the site of focused venting. All sampling techniques, containers and holding times were in accordance with the standards for water analysis as defined by the US Federal Registry (HACH, 1997). Vent water samples were collected by placing a Teflon® funnel that was connected to a 15 cm piece of Teflon® tubing over the vent (Pichler et al., 1999b). All seawater was allowed to evacuate from the funnel to minimize sample contamination with ambient seawater; subsequently 60 mL sterile syringes were then connected to the funnel/tube apparatus and filled. The intertidal vent was sampled by inserting the syringe directly in to the vent orifice. Samples were brought onshore where they were analyzed immediately for pH, oxidation–reduction potential (ORP), conductivity and total dissolved solids using a Myron-L Ultrameter™. Two samples of ambient seawater were also collected from both the northern and southern sections of the vent site and tested with the Ultrameter™. All samples were also analyzed for Fe^{2+} with a CHEMets® Fe^{2+} field kit. For this analysis, a CHEMet ampoule containing a vacuum-sealed reagent is immersed in the sample and the tip snapped off. The correct volume of sample is drawn in by vacuum. Sample and reagent are mixed by tilting the ampoule. The resulting color is then compared to color standards for quantification.

Vent fluids were then filtered to <0.45 m using a Fisher Scientific® membrane filter composed of inert mixtures of cellulose acetate and cellulose nitrate, and the samples were separated into two 60 mL high

density polyethylene bottles. One sample was left "as is" for later liquid chromatography analysis to determine major anions and for isotope analyses. The other aliquot was acidified with ultra pure HCL (1%) for subsequent lab analysis of major cations and trace metals.

Pore fluids were obtained from areas of hydrothermal sand patches (Figs. 2 and 3b) using a M.H.E PushPoint Sampler. A 60 mL syringe is connected to the device by Tygon® tubing. Markings were placed on the rod at specific insertion intervals of 10, 20 and 30 cm to sample at known depths. At the surface, samples were tested immediately for pH, ORP, conductivity and total dissolved solids with an Ultrameter® and preserved as outlined above.

Several sediment and precipitate samples were collected from around the vent site and placed into plastic containers while underwater. Once onshore, the containers were sealed with electrical tape for transport.

Two 15 cm cores were taken, one within the hydrothermal sand patch and another 3 m outside of the patch to serve as a control sample. Cores were taken by driving a sharpened 1 1/2 in. diameter PVC tube into the sediment. Once maximum depth was achieved, a sealed rubber cap was placed over the end of the tube prior to removal to form a vacuum. The PVC tubing was then slowly removed from the sediment and a second rubber cap was placed over the lower end to seal the coring tube. Onshore, the tubes were kept upright at all times while excess seawater was drained. The tubes were then cut lengthwise and split into two sections. Sediments were sampled from the core at 10 cm intervals. Photographs of the cores were taken with a digital camera and sediment colors were described using a Munsell color chart.

Gas samples were collected in GIGGENBACH sampling bottles (Giggenbach, 1975). The bottle was connected with Tygon® tubing to a funnel that was inverted over an active gas vent. The outer valve of the bottle was opened until a constant stream of gas bubbles was being emitted to reduce the possibility of seawater contamination. Following this equilibration period, the inner valve was opened and the gas sample was collected.

For comparison, seven water samples were taken from Sulfur Springs, a geothermal vent field located less than 800 m inland from Champagne Hot Springs (Fig. 1). The on-land hot springs were sampled according to procedures established for the collection of hot spring water following Nicholson (1992), then filtered and preserved as for samples from the submarine and intertidal springs.

2.2. Laboratory

Vent and pore fluids (acidified/unacidified) were kept sealed in cold storage (~3 °C) for transport to the laboratory. Chemical analyses were performed at the Center for Water and Environmental Analysis, University of South Florida, Tampa. Chloride (Cl^-), bromide (Br^-), and sulfate (SO_4^{2-}) were determined by ion chromatography using a Dionex DX500 system. Calcium, Mg, N, K, Fe, Mn, B, Si, Sr, and Li were measured by inductively coupled plasma-optical emission spectroscopy (ICP-OES) using a Perkin Elmer Optima 2000. For all vent samples, Si exists as H_4SiO_4 (Gunnarsson and Arnorsson, 2000), but will be referred to as Si for the remainder of this paper. Arsenic abundance was determined by hydride generation-atomic fluorescence spectrometry (HG-AFS) on a PSAnalytical 10.055 Millennium Excalibur instrument. Arsenic species (As^{3+} and As^{5+}) were determined by coupling ion chromatography with HG-AFS. In preparation for the total As analysis, 10 mL of each sample was mixed with 15 mL of concentrated HCl, 1 mL of saturated potassium iodide (KI) solution, and diluted with deionized water (DI) to a final volume of 50 mL. Hydrochloric acid is needed for generation of excess H^+ during HG-AFS, and KI is used to reduce all arsenic species to As^{5+} prior to analysis. $\delta^{18}O$ and δ^2H values for vent water and pore water were determined at the Colorado School of Mines stable isotope lab. For $\delta^{18}O$, 200 μL of water was equilibrated on-line with CO_2 for 12 h at 25 °C, in a GV Instruments MultiPrep preparation device. δ^2H was analyzed by continuous flow isotope ratio mass spectrometry. Samples were prepared on-line by thermal decomposition of 0.3 μL of water over chromium metal at 1050 °C in an elemental analyzer.

All sediment/precipitate samples were dried at room temperature to prevent conversion of goethite to hematite (Deer et al., 1992). General descriptions of the precipitates and sediments were made using an Olympus SZ40 Zoom stereomicroscope. Mineral identification and elemental composition were investigated with a Hitachi S-3500N variable pressure Scanning Electron Microscope (SEM) at the University of South Florida (USF) Electron Microscopy Center. The instrument includes a Robinson backscatter detector and a PGT Energy Dispersive X-ray (EDX) analysis system. A Rigaku X-ray diffractometer (XRD) was used to identify mineral phases.

To obtain bulk chemical composition for hydrothermal precipitates and CHS sediments, samples were powdered and analyzed by neutron activation analysis (NAA) by Activation Laboratories Ltd. in Ontario, Canada.

Table 1
Sample, temperature, pH and major elemental composition of Champagne Hot Springs vent waters, ambient seawater and onshore geothermal springs in mg/L

Sample	CSW1	CSW2	CSW3	CSW4	CSW5	CSW6	CSL1	Sea-water	Sulphur Springs*
Temp. (°C)	71.4	64.9	68.3	44	48.9	41.9	74	29.2	93.5
pH	5.95	6.01	6.15	6.14	6.02	5.98	6.27	7.85	4.03
Cl	9788	8968	9990	14715	13122	13851	7533	19412	73
Br	39.1	27.5	35.6	49	42.2	48.8	30.5	70.9	10.9
SO_4	1208	1111	1267	1911	1686	1805	932	2655	1096
B	11	11.4	10.9	8	8.8	8.5	12.1	4.9	8.4
Si	62.4	66.1	65	31.7	40.1	37.1	71.8	0.7	117.3
Na	5520	5080	5540	8300	7440	7700	4380	10920	140
K	206	191	210	302	276	290	160	404	9
Ca	484	474	474	482	482	478	462	474	193
Mg	584	528	594	984	864	920	392	1368	64
Li	0.75	0.76	0.73	0.49	0.57	0.53	0.77	0.18	n.d.
Mn	0.49	0.54	0.47	0.24	0.32	0.3	0.48	0.01	1.6
Fe	5.11	6.35	4.79	2.54	3.27	2.9	4.41	0	10
Sr	5.3	5.1	5.4	6.3	5.9	6.2	4.9	7.2	0.5
Sb	<0.1	<0.1	<0.1	<0.1	<0.1	<0.1	<0.1	<0.1	n.d.
Tl	<0.1	<0.1	<0.1	<0.1	<0.1	<0.1	<0.1	<0.1	n.d.
As(3+)	n.d.	80.66	79.8	14.68	n.d.	9.93	87.5	0	n.d.
As(5+)	n.d.	0	0	7.29	n.d.	8.08	2.95	2.12	n.d.
As (Total)	n.d.	80.66	79.8	21.97	n.d.	18.01	90.45	2.12	n.d.

Arsenic values are reported in μg/L.
Notes: n.d. = not determined; *Sulfur Springs values are an average of seven samples.

Gas samples were analyzed for CO_2, He, Ar, N_2, O_2, H_2, CH_4, H_2S, HCl and CO at the University of New Mexico Volcanic and Hydrothermal Fluid Analysis Laboratory. Analyses were conducted using a GOW MAC gas chromatography system specifically designed for volcanic and hydrothermal samples.

3. Results

3.1. Vent and pore fluids

Temperatures of Champagne Hot Spring vent fluids at the point of discharge were between 41 and 71.4 °C, while pH was between 5.95 and 6.15 (Table 1). The intertidal vent fluids had a temperature and pH of 74 °C and 6.27, respectively. The maximum flow rate of the submarine vents was estimated to be approximately 0.4 L/min. Vent fluids are depleted in Br^-, SO_4^{2-}, Cl^-, Na^+, K^+, and Sr^{2+} relative to ambient seawater for those elements analyzed in this study (Table 1). These species are all positively correlated with Mg^{2+}, which is also depleted relative to seawater. Chloride, for example,

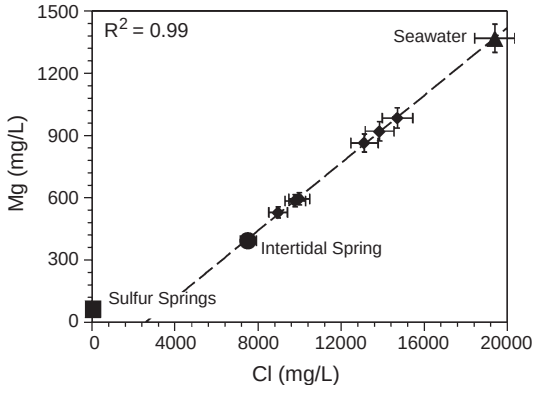

Fig. 4. Magnesium vs. Cl^- in Champagne Hot Springs vent waters, intertidal spring and seawater.

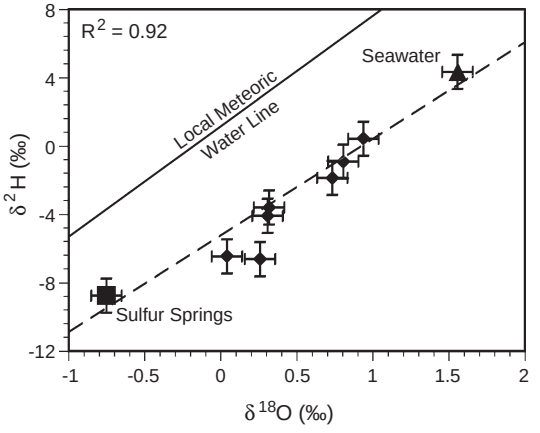

Fig. 5. Diagram showing $\delta^{18}O$ and δ^2H (both relative to VSMOW) of Champagne Hot Springs vent waters, Sulfur Springs, local precipitation and seawater. Data for the local meteoric water line from GNIP (IAEA/WMO, 2001).

Table 2
Oxygen and hydrogen isotopic compositions for Champagne Hot Springs and Sulfur Springs vent waters, seawater and average local precipitation

Sample	$\delta^{18}O$ (‰ VSMOW)	$\delta^{2}H$ (‰ VSMOW)
Sulfur Springs	−0.75	−8.7
CSL 1	0.04	−6.5
CSW 1	0.32	−3.6
CSW 2	0.26	−6.6
CSW 3	0.31	−4.1
CSW 4	0.94	0.4
CSW 5	0.73	−1.9
CSW 6	0.81	−0.9
ASW	1.56	4.3
Precipitation*	−2.15	−9.8

Notes: *Precipitation values are an average of data from the GNIP database (IAEA/WMO, 2001) over the past 25 years.

shows a high degree of correlation with Mg^{2+} (Fig. 4). Boron, Fe, As, Mn, Si and Li are all enriched relative to ambient seawater (Table 1). In all vent water samples, the CHEMets® field kit Fe^{2+} concentrations are approximately the same as those determined by ICP-OES, indicating that all of the Fe in the vent waters is present as Fe^{2+}. Sulfur Springs had a temperature of 93.5 °C and a pH of 4.03. Those elements that are enriched or depleted in Champagne Hot Springs vent fluids follow the same pattern in Sulfur Springs vent fluids. Interestingly, Ca in CHS vent fluids is approximately the same as seawater, but is depleted in Sulfur Springs vent fluids.

$\delta^{18}O$ and $\delta^{2}H$ values for vent waters compared to Vienna Standard Mean Ocean Water (VSMOW) show a mixing trend between meteorically derived vent water and seawater (Fig. 5; Table 2). Vent fluids from CSW 4, 5, and 6 have values of $\delta^{18}O$ and $\delta^{2}H$ which are most similar to that of seawater, while CSW 1, 2, 3 and the intertidal vent CSL1 have values of $\delta^{18}O$ and $\delta^{2}H$ that are increasingly negative and closer to the local meteoric water value. Sulfur Springs has $\delta^{2}H$ values that are almost identical to local meteoric water, while $\delta^{18}O$ values are still more negative than any of the vent fluids from CHS. Champagne Hot Springs vent fluids have isotopic values that lie between those of Sulfur Springs and seawater, and correlation between isotopic values from Sulfur Springs vent waters, Champagne Hot Springs vent fluids and seawater is very high ($R^2=0.92$, Fig. 5).

Pore-fluid chemistry from the hydrothermal patches is similar to the CHS vent fluid chemistry, being depleted in Br^{-}, SO_4^{2-}, Cl^{-}, Na^{+}, K^{+}, and Sr^{2+}, and enriched in B, Fe, As, Mn, Si and Li relative to ambient seawater. This is true for pore fluids from all depth intervals of the hydrothermal sand patch, and also at depth intervals of 20 and 30 cm in the control sample (Table 3). The concentrations are most similar to vent fluids from CSW 4, 5, and 6 (Tables 1 and 3). The pore fluid from the 10 cm depth at the control site is more similar to seawater chemistry.

The isotopic compositions of pore fluids follow a similar pattern as major and trace elements. Pore fluids from 10 cm in the control have values more similar to seawater, while 20 and 30 cm in the control, as well as pore fluids from all depth intervals from within the patch, are depleted in both $\delta^{18}O$ and $\delta^{2}H$ (Table 3).

Table 3
Chemical and isotopic composition and pH of pore waters from unaltered sediment (control) and hydrothermal sediment (patch)

Sample	Control (10 cm)	Patch (10 cm)	Control (20 cm)	Patch (20 cm)	Control (30 cm)	Patch (30 cm)
pH	6.84	5.91	6.47	5.90	6.63	5.86
Cl	18950	11247	12503	11182	13920	11199
Br	62.2	43.9	39.7	39.9	43.8	38.6
SO_4	2559	1477	1657	1474	1766	1470
Na	10680	6980	7380	6300	7580	6240
Mg	1358	842	916	754	934	740
K	398	262	278	244	280	238
Ca	460	406	422	410	430	406
Si	5.5	38.7	38.3	51.6	44.7	44.2
B	4.4	7.6	7.3	8.3	7.4	9.0
Fe	1.69	3.55	4.06	3.90	4.23	4.22
Mn	0.12	0.84	0.83	0.99	0.84	1.01
Sr	7.1	5.4	5.7	5.2	5.9	5.1
Li	0.18	0.46	0.46	0.53	0.46	0.52
$\delta^{18}O$	1.26	n.d.	.49	n.d.	.59	n.d.
$\delta^{2}H$	2.4	n.d.	−3.5	n.d.	−1.6	n.d.

Values for chemical parameters are in mg/L and in ‰ (VSMOW) for oxygen and hydrogen isotopes.
Notes: n.d. = not determined.

Table 4
Chemical composition in ppm of Champagne Hot Springs hydrous ferric oxide (HFO) precipitates compared to average Caribbean seafloor sediments

Sample	CSP1	CSP2	CSP3	CSP4	CSP5	CSP6	*Carib. sediment
Fe	344000	268000	276000	328000	326000	231000	28100
Mn	80	60	35	20	65	70	1641
S	935	610	665	485	1395	535	n.d.
Na	15700	14400	14400	13800	28100	18400	20900
As	1610	1120	1070	1620	1880	993	<0.1
Br	65	39	40	41	177	46	n.d.
Sb	22.2	27.3	39	25.7	36.9	20.7	<0.1
Co	0	0	0	0	7	6	13.5
Cs	5	7	8	11	4	8	n.d.
Sc	0.8	2.9	3	3	1.4	5.9	n.d.
La	3	4	4	4	3	6	15.5
Ce	7	11	8	9	0	11	n.d.
Sm	1.6	1.6	2.1	1.9	1.8	1.8	n.d.
Yb	2.2	2.5	3	3.4	1.6	2.4	n.d.
Lu	0.33	0.37	0.47	0.52	0.24	0.37	n.d.
Eu	0.4	<0.1	0.4	0.6	<0.1	0.6	n.d.

Notes: n.d. = not determined; *Caribbean Sediments = average Caribbean seafloor sediment from the entire Lesser Antilles from Johnson and Cronan (2001).

3.2. Hydrothermal precipitates, sediments and cores

Hydrothermal precipitates and sediments are enriched in Na, Fe, As and Sb, and depleted in Mn when compared to values for Caribbean sediments (Tables 4 and 5). In the hydrothermal precipitates Fe and As are markedly enriched, with maximum concentrations of 38.75% Fe and 1880 ppm As. In comparison to Caribbean sediments, Fe is enriched over 13-fold and As is enriched over 1000-fold. Fe and As show a high degree of correlation, with an R^2 value of 0.97 (Fig. 6). Sediment samples are also considerably enriched in Fe and As in comparison to typical Caribbean sediments, with maximum concentrations of 12.0% Fe and 311 ppm As (Table 5). In particular Sb and As were elevated, with enrichment factors of 10 and 100-fold, respectively. Fe and As in sediments, as with precipitates, show a high degree of positive correlation, with an R^2 value of 0.95 (Fig. 6).

Scanning electron microscopy analyses of the hydrothermal precipitates showed that they consist of small spherical bodies, approximately 2 μm in diameter. This observation is in good agreement with the morphology observed for synthesized and natural two-line

Table 5
Chemical composition in ppm of Champagne Hot Springs hydrothermally influenced sediments compared to average Caribbean seafloor sediments

Sample	CS1	CS2	CS3	CS4	CS5	CS8	CS10	Carib. sediment
Fe	106000	78900	120000	821000	43700	109000	92000	28100
Mn	140	120	60	85	160	130	65	1641
S	440	305	5450	1055	390	265	590	n.d.
Na	25600	30300	55400	31900	24400	28000	28200	20900
As	54	100	311	114	38	223	309	<0.1
Br	44	63	496	135	12	50	37	n.d.
Sb	1.2	3.5	10.7	2.3	0.7	7.6	4.6	<0.1
Co	31	19	21	22	11	14	10	13.5
Cs	5	5	4	4	2	8	5	n.d.
Sc	26.6	17.3	14	18.2	13.2	14.7	11.9	n.d.
La	10	11	7	10	10	11	14	15.5
Ce	24	22	15	23	21	24	29	n.d.
Sm	2.7	2.2	2.3	2.4	2.5	2.3	2.8	n.d.
Yb	2.7	1.9	2.8	2	1.9	2.1	2.1	n.d.
Lu	0.41	0.3	0.42	0.31	0.29	0.32	0.32	n.d.
Eu	0.6	0.9	<0.1	0.6	0.7	0.7	0.8	n.d.

Notes: n.d. = not determined; *Caribbean Sediments = average Caribbean seafloor sediment from the entire Lesser Antilles from Johnson and Cronan (2001).

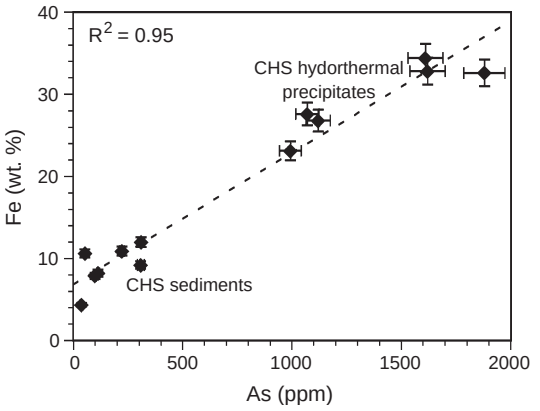

Fig. 6. Arsenic vs. Fe in Champagne Hot Springs hydrous ferric oxide precipitates and sediments.

hydrous ferric oxide (HFO or ferrihydrite) (e.g., Janney et al., 2000; Pichler et al., 1999c).

X-ray diffraction analysis of the precipitates confirmed the presence of two-line ferrihydrite (Fig. 7). The high concentration of Si in the vent fluids is also reflected in the EDX analysis of the hydrothermal precipitates, and indicates incorporation of silica into the HFO. Studies have indicated that silicate compounds can inhibit further crystallization, resulting in a poorly crystalline surface morphology (Boyd and Scott, 1999; Schwertmann, 1966, 1970).

Two sediment cores, one from within and one from outside of the hydrothermal sand patch, were compared. The core from within the hydrothermal sand patch shows abundant HFO coatings on sediment grains. At 10–20 cm depth the hydrothermal patch core also contained dark orange to rust colored HFO precipitates that are rounded and average approximately 0.2–0.5 cm in diameter. The control core did not show any HFO coatings or precipitates, even though the pore-waters indicated some hydrothermal influence.

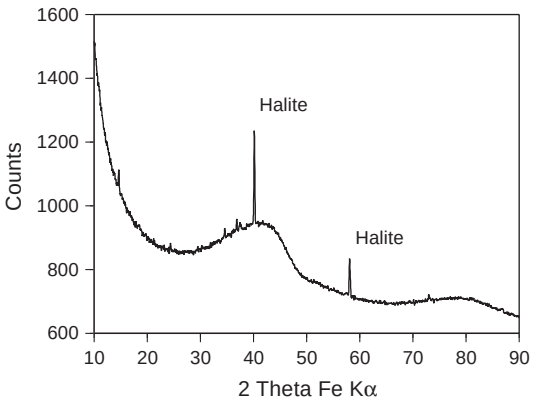

Fig. 7. X-ray diffraction pattern for a typical Champagne Hot Springs hydrous ferric oxide (HFO) sample. The presence of the halite peaks is an artifact caused by drying, i.e., halite precipitation due to the evaporation of seawater trapped in the sample.

Table 6
Composition of Champagne Hot Springs gas samples in mmol/mol dry gas

Sample	1	2	3	4
CO_2	837	934	741	842
H_2S	42.5	16.4	28.1	39.4
HCl	<4.2	<1.6	<2.7	<3.8
He	0.03	0.01	0.02	0.03
H_2	0.01	0.00	0.02	0.00
Ar	1.3	0.8	4.7	1.8
O_2	1.2	0.8	4.5	1.1
N_2	110	44	211	107
CH_4	4.0	1.5	7.2	3.9
CO	<0.0008	<0.0003	<0.0005	<0.0007
He/Ar	0.02	0.01	0.01	0.02
N_2/Ar	86	54	45	61
N_2/He	3721	4013	13486	3897
CH_4/CO_2	0.005	0.002	0.010	0.005

3.3. Gases

All Champagne Hot Springs gas samples have CO_2 as the major constituent, accounting for 74–93% by volume of the total analyzed gas (Table 6). Nitrogen (N_2) is the second most abundant gas, with values ranging from 4% to 21% by volume. Hydrogen sulfide (H_2S) comprises 1.6–3.9% of the total gas volume, while CH_4, HCL, O_2 and Ar have minor concentrations of 0.15, 0.73%, 0.07, and 0.46% by volume, respectively. The trace gas constituents, He, H_2 and CO, range from 0.0% to 0.003% of the total gas volume. Minimum and maximum gas flux, as determined by fluid displacement by gas, were 0.1–0.4 L/min, respectively.

4. Discussion

4.1. Origin and mixing trend of vent waters

Fluids within a shallow-water submarine hydrothermal system may be derived from any one or a combination of the following sources: meteoric water, seawater, connate water and magmatic water (e.g., Nicholson, 1992; Pichler, 2005; Pichler et al., 1999b). Mixing of waters from different sources can directly affect the chemical and isotopic composition, temperature profile and gas content of hydrothermal fluids. Active deep-sea hydrothermal systems along mid-oce-

anic ridges, in back-arc basins and on the flanks of seamounts most likely derive all of their fluid from seawater. In contrast, on-land hydrothermal systems derive most of their fluids from meteoric sources along with possible magmatic contributions (e.g., Giggenbach, 1992). Understanding the origin of hydrothermal fluids is an important step in deciphering subsurface processes and reservoir conditions.

Contrary to Johnson and Cronan (2001), who suggest that offshore hot springs of the Lesser Antilles, including Dominica, are fed by a seawater dominated hydrothermal fluid, we suggest that the vent fluid at Champagne Hot Springs is likely a mixture of meteorically derived hydrothermal fluid and seawater in varying proportions. Entrainment of ambient seawater occurs in the shallow sub-seafloor, and possibly during sampling. The proportion of each of these two proposed endmembers is dependent upon the flow rate and temperature at each individual vent. Vents 1, 2 and 3 have significantly higher flow rates and temperatures relative to vents 4, 5, and 6. Similarly, vents 1, 2, and 3 contain lower concentrations of major seawater constituents (Cl^-, Br^-, SO_4^-, Na^+, Mg^{2+}, and K^+) while vents 4, 5, and 6 exhibit higher concentrations of these species (Table 1). It is assumed that lower flow rates will result in greater entrainment of ambient seawater (Dando et al., 2000; Robinson et al., 1997). Previous research at Champagne Hot Springs has also shown that increased flow rates and temperatures at the vent field results in a fluid that contains less major seawater constituents (Johnson and Cronan, 2001). Molecular ratios, such as Cl/Mg, Cl/Br and Cl/SO_4, are approximately the same as those caused by seawater mixing (Nicholson, 1992).

The major species Br^-, SO_4^{2-}, Na^+, K^+ along with As and Li in Champagne Hot Springs vent fluids show the same high degree of correlation with Mg^{2+} as does Cl^- in Fig. 4 ($R^2 > 0.99$). Only Fe and Mn have lower R^2 values of 0.67 and 0.87, respectively, which may be caused by the difference in environmental conditions between the on-land vent and the submarine vents. The intertidal vent CSL1 contains the lowest relative concentrations of major seawater constituents (Cl^-, Br^-, SO_4^{2-}, Na^+, K^+, Mg^{2+}) of all Champagne Hot Spring vent fluids, it is likely to have the least amount of seawater mixing. Seawater mixing can occur during sampling, in the shallow subsurface and at depth, and these conditions are more likely to occur in the submarine vents. Although the atmosphere contains much more O_2 relative to that dissolved in the surface seawater, diffusion of O_2 in the hydrothermal fluids will occur very slowly, and mixing with oxygen-rich seawater becomes much more important. Therefore, decreased mixing of oxygen-rich seawater in the subaerial vent results in less oxidation of Fe^{2+} and Mn^{2+}, subsequently diminishing precipitation. The result is a subaerial vent fluid (CSL1) with higher relative concentrations of Fe and Mn versus Mg^{2+} values (Table 1).

Assuming conservative behavior during mixing, chemical tracers can provide insights into the mixing process given sufficient variation in concentration of the tracer between seawater and the hydrothermal fluid (Edmond et al., 1979; Pichler, 2005; Pichler et al., 1999b). The ideal situation is to employ a tracer that is essentially absent in one of the mixing partners. To correct for seawater mixing, this study employs the use of Cl^- as a conservative tracer and Si as an indicator of hydrothermal fluid input (e.g., Sedwick and Stüben, 1996), since Cl^- is essentially absent in the meteorically derived hydrothermal fluids at Sulfur Springs and Si is at a near-zero concentration in ambient seawater. As stated previously, likely sources of near shore hydrothermal submarine vent fluids in regions of steep topography can be meteoric water or seawater, depending on the location of the Ghyben–Herzberg boundary (i.e., subsurface boundary between seawater and meteoric water) (e.g., Chuck, 1967; Nahm, 1966). Fig. 8 contains two Si vs. Cl^- plots overlain on each other. One plot includes the data points for Champagne Hot Springs, intertidal spring, Sulfur Springs and seawater. The second series contains only the data points for Champagne Hot Springs.

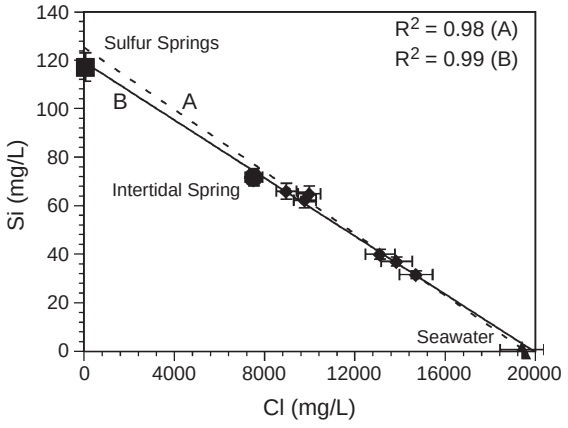

Fig. 8. The Cl^- vs. Si trend for seawater, Champagne Hot Springs waters and the meteoric derived hydrothermal fluids of Sulfur Springs. The figure contains two different linear regression lines: (A) Champagne Springs vent waters only (dashed) and (B) all data points (solid). The close agreement between the two linear regressions indicates that the variation seen in Champagne Springs vent waters is due to mixing between Sulfur Springs and seawater at varying proportions.

The trend lines (linear regressions) are plotted for each data series separately, with the solid line representing all of the data points and the dashed line pertaining only to the vent water samples. The purpose of the separate trend lines is to show that the Sulfur Springs and seawater data points do not serve as outlying anchor points for the vent water samples; both trend lines are almost identical and are highly correlated with R^2 values of 0.98 and 0.99. This strongly suggests the mixing endmembers for discharging fluids at Champagne Hot Springs vent sites are the meteorically derived Sulfur Springs hydrothermal fluids and seawater.

The $\delta^{18}O$ and $\delta^{2}H$ values of Champagne Hot Springs vent waters also suggest mixing between Sulfur Springs and seawater (Table 2). Linear regression plots show that the isotopic composition of the vent waters are on a mixing line between these two endmembers, and that the Sulfur Springs samples are most similar in isotopic composition to that of average local precipitation (Fig. 5). For Sulfur Springs, the difference in $\delta^{18}O$ from meteoric water may be due to fractionation during high-temperature water–rock interaction. The positive shift in $\delta^{18}O$ for seawater relative to VSMOW may be due to surface evaporation. Since the vent waters are mixtures between these two endmembers, it is expected that their $\delta^{18}O$ values should also be shifted towards more positive values.

4.2. Pore waters in the hydrothermal sand patches

The compositions of pore-water samples within the hydrothermally altered sand patches at Champagne Hot Springs are also consistent with mixtures, in varying proportions, of meteorically derived hydrothermal fluid and seawater. Higher than ambient temperatures of 44 °C inside the colored patches (Fig. 3b) combined with upward flow of a metal-rich, low-pH fluid through the sediment indicate a hydrothermal origin and influence (Table 3). Stepping away from the patches the temperatures rapidly decrease to that of ambient seawater (29 °C) and upward flow of the hydrothermal fluid is not evident at the surface. However, those pore water profiles that were taken outside the colored patches show some hydrothermal influence at depth (Table 3). This same process accounts for the relative percentage of mixing between hydrothermal fluid and seawater; sustained heat flow results in rapid ascent and less seawater entrainment. At lower temperatures, downward diffusion of seawater becomes increasingly significant and results in increased seawater mixing (e.g., Dando et al., 2000; Robinson et al., 1997). This indicates that the colored patches are likely sand covered vents that discharge from fractures and fissures, as indicated by their elongated form (Fig. 3b). The chemistry of the Champagne Hot Springs pore fluids is consistent with the process mentioned above. Pore waters from the patch area located immediately above the vent have approximately the same concentrations of Fe, Mn and Si at all depth intervals (10, 20 and 30 cm). This indicates that in the patch area there is little mixing with seawater during ascent, since seawater values of Fe, Mn and Si are low. This observation is also supported by the relatively constant proportions of Cl^-, Br^-, SO_4^{2-}, Na^+, K^+, Mg^{2+} and Ca^{2+} in the patch fluids at all depths. This suggests that sustained heat flow and limited seawater mixing in the immediate vicinity of the patch vent maintain reducing conditions during fluid ascent. A change in physico-chemical conditions in the upper 10 cm caused by mixing with seawater causes the precipitation of HFO (e.g., Pichler and Veizer, 1999). In the control core (away from the vent) a greater seawater influence already lower in the core seemingly prevents the precipitation of HFO at or near the sediment surface.

4.3. Gas chemistry

Gas samples at Champagne Hot Springs are predominately CO_2 (~74–93%; Table 6). In most submarine or subaerial hydrothermal systems, CO_2 is the most abundant gas, typically representing over 85% of the total gas content at discharge (e.g., Forrest et al., 2005; Mahon et al., 1980). Carbon dioxide gas can be produced by thermal alteration of carbonate rocks and minerals, breakdown of organic matter, magmatic inputs, and solutes in meteoric waters (Nicholson, 1992).

The second major component of Champagne Hot Springs gases is nitrogen (N_2). Gases containing higher concentrations of N_2 and lesser amounts of He and Ar are typical of arc-type settings as expected for Dominica (Fischer et al., 1997). Some N_2 could also be of atmospheric origin, introduced due to seawater–gas interaction in the shallow subsurface. However, the O_2/N_2 ratios are too small (0.01 vs. 0.25, Table 6) for a significant atmospheric contribution (Pichler et al., 1999a). The samples also have N_2/He ratios between ~1000 and 14,000 and N_2/Ar ratios ~45–86, which are also typical of arc-type gases (e.g., Brown, 2002). N_2 input into a hydrothermal system can be either or both dissolved constituents in meteoric water and of magmatic origin. The N_2/Ar ratios for Champagne Hot Springs gases (45–86) are elevated above

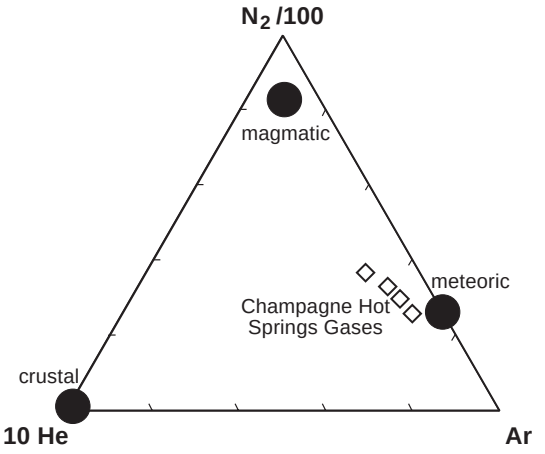

Fig. 9. Ternary plot of relative N_2, He and Ar concentrations that are used to identify gas source, i.e., crustal, magmatic or meteoric (after Giggenbach, 1991). Champagne Hot Springs gas samples show a mainly meteoric source with varying amounts of magmatic gas.

those of meteoric water (38), suggesting a magmatic input. As previously argued in the discussion about vent water, there appears to be a clear input of meteoric water to the Champagne Hot Springs system. Therefore, it is likely there is also input of N_2 dissolved in meteoric water.

Combined, the elevated CO_2 concentrations, along with N_2/Ar and N_2/He molecular ratios, suggest both magmatic and meteoric gas contributions, as is shown in Fig. 9. (e.g., Giggenbach, 1980).

4.4. Formation and chemistry of precipitates/sediments

Alteration of Fe-rich minerals and direct precipitation from solution are two processes that lead to the formation of hydrous ferric oxide (Murray, 1979). These reactions can be enhanced by microbial and/or bacterial activity (e.g., Ehrlich, 1995). Its formation is dependent upon a combination of various environmental conditions such as pH, Eh, temperature, precipitation rate and Fe concentration (Binns et al., 1993; Fortin et al., 1993; Hekinian et al., 1993). Direct precipitation from solution can occur by slow hydrolysis of Fe^{3+} or by oxidation of Fe^{2+}-rich fluids (Murray, 1979). Concentrations of Fe^{2+} measured during field analysis were the same as those for total Fe, measured in the lab by ICP-OES. This indicates that Fe^{3+} is absent in Champagne Hot Springs vent fluids and that precipitation occurs by oxidation of Fe^{2+} through mixing with cool, alkaline, oxygenated seawater (Millero et al., 1987). Mixing of Champagne Hot Springs vent fluids (Eh ~0.04 v and pH ~6.0) and seawater (Eh ~0.13 v and pH ~8.0) increases both Eh and pH while lowering temperature. These conditions are suitable for the precipitation of hydrous ferric oxide (Pichler and Veizer, 1999).

The chemistry of the Champagne Hot Springs precipitates and sediments reflects all of the previously mentioned processes (Tables 4 and 5). The only exception is the enrichment of Na^+ due to the precipitation of halite during drying of the samples. The marked enrichment of Fe and Mn in both the precipitates and sediments reflects their relatively high concentrations in the vent fluids.

In Table 4, the range of Fe concentrations in the precipitates (from 23% to 39%) is a function of location and proximity to focused venting. The precipitate with the highest Fe concentration (CSP 4) is located in the immediate vicinity (<1 m) of vent CSW 2, the vent with the highest Fe concentration in the fluid (Table 1). Decreasing Fe concentrations in the precipitates correlates with their location at vents having lower relative Fe concentration in the fluid. Iron concentrations in the sediments also decrease with increasing distance from the vents. The correlation between Fe concentrations and locations in both the sediments and the precipitates again suggests rapid precipitation of hydrous ferric oxides by mixing of Fe^{2+} rich vent fluid with oxygenated seawater (Millero et al., 1987).

The high As concentrations in the hydrothermal precipitates and sediments are caused by a combination of elevated As in the vent fluids and the scavenging capacity of HFO, which is well documented (e.g., Pichler et al., 1999c; Hering et al., 1997). In aqueous systems, scavenging of elements by metal hydroxides results from: (1) coprecipitation, (2) adsorption, (3) surface complex formation, (4) ion exchange and (5) penetration of the crystal lattice (Chao and Theobald, 1976). Adsorption has been observed to be the source of most surface chemical reactions, making it the most likely process responsible for the minor and trace element chemistry of Champagne Hot Springs precipitates and sediments (Stumm and Morgan, 1996). Relative to arsenic, minor element concentrations are low and reflect their low concentrations in the vent fluids (Table 1).

The SEM, EDX and XRD analyses all indicate the precipitates at Champagne Hot Springs are a 2-line ferrihydrite. Fig. 6 demonstrates the high degree of correlation between Fe and As in the Champagne Hot Springs precipitates and sediments. Arsenic and hydrous ferric oxide associations occur in a variety of natural environments (Belzile and Tessier, 1990; Boyle and Jonasson, 1973; O'Neill, 1990; Parker and Nicholson, 1990).

The role of microbes in the formation of ferrihydrite in shallow-water hydrothermal systems has not been

extensively studied. However, it is known that Fe^{2+} is easily oxidized in seawater, and thus its precipitation as Fe^{3+} can be considered largely abiotic (e.g., Millero et al., 1987). Arsenic, on the other hand, does not seem to oxidize as rapidly as Fe(II) in seawater. Recent data from the Ambitle hydrothermal system show that As^{3+} remained up to several days in seawater (Price and Pichler, 2005). In other words, sluggish oxidation kinetics, which is generally required for microbes to extract metabolic energy, may point to microbial involvement in As-oxidation here. The presence of As^{5+} in ferrihydrite is consistent with at least partial microbial oxidation of As^{3+}. Whether microbially mediated or purely abiotic, oxidation of As^{3+} to As^{5+} is a necessary step prior to sorption. At the pH and temperature conditions in the CHS vent water, As^{3+} is the dominant species (Table 1) and exists as uncharged H_3AsO_3, limiting its potential for adsorption onto ferrihydrite (e.g., Clifford and Ghurye, 2002).

5. Conclusions

Geochemical analysis of vent fluids, precipitates, gas, and sediments from the Champagne Hot Springs vent field suggests that:

1. Vent waters/pore waters are mixtures of seawater and meteoric derived hydrothermal fluid in varying proportions.
2. Precipitates and volcaniclastic sediment coatings are hydrous ferric oxide and reflect elevated concentrations of Fe in the vent fluids. Elevated arsenic concentrations reflect adsorption on hydrous ferric oxide.
3. Hydrothermal sand patches are present in areas where upward flow of hot hydrothermal fluid induces precipitation of hydrous iron oxides at or near the sediment/seawater interface. Hydrothermal discharge from this area is very similar in composition to the CHS vent water.
4. Venting gases are likely of meteoric and magmatic origin and are typical of arc-type settings.

Acknowledgements

We thank the Dominica Department of Fisheries and particularly department head Andrew Magloire. Kevin McCarthy thanks the Latin American and Caribbean Studies Center at USF, the Geological Society of America and American Association of Petroleum Geologists for providing funding for this research. We thank Dr. Tobias Fischer (University of New Mexico) for the gas analyses and Dr. John Humphrey (Colorado Scholl of Mines) for the isotope analyses. The reviews by two anonymous reviewers helped to improve the final version of this manuscript. **[PD]**

References

Belzile, N., Tessier, A., 1990. Interactions between arsenic and iron oxyhydroxides in lacustrine sediments. Geochimica Cosmochimica Acta 54, 103–109.

Binns, R.A., Scott, S.D., Bogdanov, Y.A., Lisitzin, A.P., Gordeev, V.V., Gurvich, E.G., Finlayson, E.J., Boyd, T., Dotter, L.E., Wheller, G.E., Muravyev, K.G., 1993. Hydrothermal oxide and gold-rich sulfate deposits on Franklin Seamount, western Woodlark Basin, Papua New Guinea. Economic Geology 88, 2122–2153.

Boyd, T., Scott, S.D., 1999. Two-XRD-line ferrihydrite and Fe–Si–Mn oxyhydroxide mineralization from Franklin Seamount, western Woodlark Basin, Papua New Guinea. Canadian Mineralogist 37 (4), 973–990.

Boyle, R.W., Jonasson, I.R., 1973. The geochemistry of arsenic and its use as an indicator element in geochemical prospecting. Journal of Geochemical Exploration 2, 251–296.

Brown, L.K., 2002. Gas Geochemistry of the Volcanic Hydrothermal Systems of Dominica and St. Lucia, Lesser Antilles: Implications for Volcanic Monitoring. University of New Mexico.

Chao, T.T., Theobald, J.P.K., 1976. The significance of secondary iron and manganese oxides in geochemical exploration. Economic Geology 71, 1560–1569.

Chuck, R.T., 1967. Groundwater resources development on tropical islands of volcanic origin. Int. Conf. Water for Peace, Washington, D. C., pp. 963–970.

Clifford, A.D., Ghurye, G.L., 2002. Metal-oxide adsorption, ion exchange, and coagulation–microfiltration for arsenic removal from water. In: Frankenberger Jr., W.T. (Ed.), Environmental Chemistry of Arsenic. Marcel Dekker, New York, pp. 217–245.

Dando, P.R., Leahy, Y., 1993. Hydrothermal activity off Milos. Hellenic Volcanic Arc. BRIDGE, 20–21.

Dando, P.R., Aliani, S., Arab, H., Bianchi, C.N., Brehmer, M., Cocito, S., Fowler, S.W., Gundersen, J.K., Hooper, L.E., Kolbl, R., Kuever, J., Linke, P., Makropoulos, K.C., Meloni, R., Miquel, J.C., Morri, C., Muller, S., Robinson, C., Schlesner, H., Sievert, S., Stohr, R., Stuben, D., Thomm, M., Varnavas, S.P., Ziebis, W., 2000. Hydrothermal studies in the Aegean Sea. Physics and Chemistry of the Earth 25 (1), 1–8.

Deer, W.A., Howie, R.A., Zussmann, J., 1992. An introduction to the rock-forming minerals. Longman Scientific and Technical, 696.

Edmond, J.M., Jacobs, S.S., Gordon, A.L., Mantyla, A.W., Weiss, R.F., 1979. Water column anomalies in dissolved silica over opaline pelagic sediments and the origin of the deep silica maximum. Journal of Geophysical Research—Oceans and Atmospheres 84 (NC12), 7809–7826.

Ehrlich, H.L., 1995. Geomicrobiology. Marcel Dekker, Inc., New York. 720 pp.

Fink, L.K.J., 1972. Bathymetric and geologic studies of the Guadeloupe region, Lesser Antilles island arc. Marine Geology 12 (4), 267–288.

Fischer, T.P., Sturchio, N.C., Stix, J., Arehart, G.B., Counce, D., Williams, S.N., 1997. The chemical and isotopic composition of fumarolic gases and spring discharges from the Galeras Volcano, Colombia. Journal of Volcanology and Geothermal Research 77, 229–253.

Forrest, M.J., Ledesma-Vázquez, J., Hilton, D.R., 2005. Gas geochemistry of a shallow submarine hydrothermal vent associated with the El Requesón fault zone, Bahía Concepción, Baja California Sur, México. Chemical Geology 57, 82–95 (this issue).

Fortin, D., Leppard, G.G., Tessier, A., 1993. Characteristics of lacustrine diagenetic iron oxyhydroxides. Geochimica Cosmochimica Acta 57, 4391–4404.

Giggenbach, W.F., 1975. A simple method for the collection and analysis of volcanic gas samples. Bulletin of Volcanology 36, 132–145.

Giggenbach, W.F., 1980. Geothermal gas equilibria. Geochimica Cosmochimica Acta 44, 2021–2032.

Giggenbach, W.F., 1991. Chemical techniques in geothermal exploration. In: D'Amore, F. (Ed.), Application of Geochemistry in Geothermal Reservoir Development. UNITAR/UNDP, Rome, pp. 495–510.

Giggenbach, W.F., 1992. Isotopic shifts in waters from geothermal and volcanic systems along convergent plate boundaries and their origin. Earth and Planetary Science Letters 113 (4), 495–510.

Gunnarsson, I., Arnorsson, S., 2000. Amorphous silica solubility and the thermodynamic properties of $H_3SiO_4^\circ$ in the range of 0° to 350° at Psat. Geochimica Cosmochimica Acta 64 (13), 2295–2307.

Hach Company,, 1997. Water Analysis Handbook. Loveland, Colorado. 1312 pp.

Heikoop, J.M., Tsujita, C.J., Risk, M.J., Tomascik, T., Mah, A.J., 1996. Modern iron ooids from a shallow-marine volcanic setting: Magengetang Indonesia. Geology 24, 759–762.

Hekinian, R., Bideau, D., Francheteau, J., Cheminee, J.L., Armijo, R., Lonsdale, P., Blum, N., 1993. Petrology of the East Pacific rise crust and upper mantle exposed in Hess Deep (eastern equatorial Pacific). Journal of Geophysical Research 98, 8069–8094.

Hering, J.G., Chen, P.-Y., Wilkie, J.A., Elimelech, M., 1997. Arsenic removal from drinking water during coagulation. Journal of Environmental Engineering, 800–807.

Hodkinson, R.A., Cronan, D.S., Varnavas, S., Perissoratis, C., 1994. Regional geochemistry of sediments from the Hellenic volcanic arc in regard to submarine hydrothermal activity. Marine Georesources and Geotechnology 12, 83–129.

International Atomic Energy Agency/World Meteorological Organisation, 2001. Global Network of Isotopes in Precipitation (GNIP). Database accessible at: http://isohis.iaea.org.

Janney, D.E., Cowley, J.M., Buseck, P.R., 2000. Transmission electron microscopy of synthetic 2- and 6-line ferrihydrite. Clays and Clay Mineral 48, 111–119.

Johnson, A., Cronan, D.S., 2001. Hydrothermal metalliferous sediments and waters off the Lesser Antilles. Marine Georesources and Geotechnology 19, 65–83.

Lindsay, J.M., Stasiuk, M.V., Shepherd, J.B., 2003. Geological history and potential hazards of the late-Pleistocene to Recent Play Pays volcanic complex, Dominica, Lesser Antilles. Bulletin of Volcanology 65 (2–3), 201–220.

Mahon, W.A.J., McDowell, G.D., Finlayson, J.B., 1980. Carbon dioxide: its role in geothermal systems. New Zealand Journal of Science 23, 133–148.

Martin-Kaye, P.H.A., 1969. A summary of the geology of the Lesser Antilles. Overseas Geology and Mineral Resources 10, 172–206.

Millero, F.J., Sotolongo, S., Izaguirre, M., 1987. The oxidation kinetics of Fe(II) in seawater. Geochimica Cosmochimica Acta 51, 793–801.

Murray, J.W., 1979. Iron oxides. In: Burns, R.G. (Ed.), Marine Minerals. Mineralogical Society of America, Washington, pp. 47–98.

Nahm, G.-Y., 1966. Geology and groundwater resources of volcanic island, Cheju-do. Geology and Ground-Water Resources 3, 109–133.

Nicholson, K., 1992. Geothermal Fluids. Springer Verlag, p. 266.

O'Neill, P., 1990. Arsenic. In: Pacey, G.E., Ford, J.A. (Eds.), Heavy Metals in Soils. Blackie, Glasgow, pp. 83–99.

Parker, R.J., Nicholson, K., 1990. Arsenic in geothermal sinters: determination and implications for mineral exploration. In: Harvey, C.C., Browne, P.R.L., Freestone, D.H., Scott, G.L. (Eds.), 12th NZ Geothermal Workshop. Auckland University, Auckland, pp. 35–39.

Pichler, T., 2005. Stable and radiogenic isotopes as tracers for the origin, mixing and subsurface history of fluids in shallow-water hydrothermal systems. Journal of Volcanology and Geothermal Research 139 (3–4), 211–226.

Pichler, T., Dix, G.R., 1996. Hydrothermal venting within a coral reef ecosystem, Ambitle Island, Papua New Guinea. Geology 20 (5), 435–438.

Pichler, T., Veizer, J., 1999. Precipitation of Fe(III) oxyhydroxide deposits from shallow-water hydrothermal fluids in Tutum Bay, Ambitle Island, Papua New Guinea. Chemical Geology 162, 15–31.

Pichler, T., Giggenbach, W.F., McInnes, B.I.A., Buhl, D., Duck, B., 1999a. Fe-sulfide formation due to seawater–gas–sediment interaction in a shallow water hydrothermal system at Lihir Island, Papua New Guinea. Economic Geology 94, 281–288.

Pichler, T., Veizer, J., Hall, G.E.M., 1999b. The chemical composition of shallow-water hydrothermal fluids in Tutum Bay, Ambitle Island, Papua New Guinea and their effect on ambient seawater. Marine Chemistry 64, 229–252.

Pichler, T., Veizer, J., Hall, G.E.M., 1999c. Natural input of arsenic into a coral-reef ecosystem by hydrothermal fluids and its removal by Fe(III) oxyhydroxides. Environmental Science and Technology 33 (9), 1373–1378.

Price, R.E., Pichler, T., 2005. Distribution, speciation and bioavailability of arsenic in a shallow-water submarine hydrothermal system, Tutum Bay, Ambitle Island, PNG. Chemical Geology 224, 122–135 (this issue).

Robinson, C., Ziebis, W., Miller, S., Eichstadt, K., Dando, P.R., Linke, P., Varnavas, S.P., Megalovasilis, P., Panagiotaras, D., 1997. In situ investigations of shallow water hydrothermal systems, Palaeochori Bay, Milos, Aegean Sea. Fourth Underwater Science Symposium, The Society for Underwater Technology, Newcastle Upon Tyne, pp. 85–100.

Schwertmann, U., 1966. Die Bildung von Eisenoxidmineralien. Fortschritte der Mineralogie 46, 274–285.

Schwertmann, U., 1970. Der Einfluss einfacher organischer Anionen auf die Bildung von Goethit und Haematit aus amorphen Fe(III) hydroxid. Geoderma 3, 207–214.

Sedwick, P., Stüben, D., 1996. Chemistry of shallow submarine warm springs in an arc-volcanic setting: Vulcano Island, Aeolian Archipelago, Italy. Marine Chemistry 53, 146–161.

Sigurdsson, H., Shepherd, J.B., 1974. Amphibole-bearing basalts from the submarine volcano Kick'em-Jenny in the Lesser Antilles island arc. Bulletin of Volcanology 38, 891–910.

Stumm, W., Morgan, J.J., 1996. Aquatic Chemistry. Wiley-Interscience, New York, p. 1022.

UNEP/IUCN, 1988. Dominica. In: Wells, S.M. (Ed.), Coral Reefs of the World. Volume 1: Atlantic and Eastern Pacific. IUCN, Gland, Switzerland; UNEP, Nairobi, Kenya; and Cambridge, U.K. 137 pp.